

# Interpretation of drill core and georadar data of coarse gravel deposits

Christian Regli<sup>a</sup>, Peter Huggenberger<sup>a,\*</sup>, Martin Rauber<sup>b</sup>

<sup>a</sup>Department of Earth Sciences, Applied and Environmental Geology, University of Basel, Bernoullistr. 16, 4056 Basel, Switzerland

<sup>b</sup>Rauber Consulting, Technopark, Technoparkstr. 1, 8005 Zürich, Switzerland

Received 13 November 2000; revised 29 August 2001; accepted 25 September 2001

## Abstract

Pollution in the shallow subsurface has led to an increasing need of understanding how to quantitatively characterize both the heterogeneity of gravel aquifers and the influence of heterogeneity on groundwater flow and solute transport. Models play an important role in decision-making processes, especially in the context of better characterizing and in forecasting the behavior of a given geological system. The objective of the present paper is the derivation of a gradual lithofacies-based interpretation of outcrop, drill core, and ground penetrating radar (GPR or georadar) data of different quality. The presented method allows a probability estimation of drill core layer descriptions and radarfacies types representing defined sedimentary structure types. The method includes a determination of 'initial structure type probabilities' for grain-size categories and combinations thereof described in drill core layer descriptions as well as a subsequent differentiation of these structure type probabilities in an iterative process considering 'additional information' like main constituent, quantity, fraction, and sorting of single grain-size categories, color, chemical precipitation, layer thickness, and adjacent layer. The radarfacies types are calibrated with drill cores located in the vicinity of georadar sections. The calibration process consists of the assignment of the calculated structure type probabilities from the drill core layer descriptions to the corresponding radarfacies types considering the proportion in thickness between drill core layers and georadar structures. The structure type probabilities can be given for points along boreholes and a grid with arbitrary mesh size along georadar sections. The method is applied to field examples from the Rhine/Wiese aquifer near Basel in Switzerland. The resulting structure type probabilities can be used for conditioning stochastic simulations of geological models. However, the conditioned stochastic simulation of the Rhine/Wiese aquifer is the topic of another paper. The results show the importance of a detailed sedimentological analysis of outcrops and drill cores as well as its significance on the distinction of sedimentary structure types. © 2002 Elsevier Science B.V. All rights reserved.

**Keywords:** Drill core analysis; Ground penetrating radar; Aquifer stratigraphy; Site characterization; Heterogeneity; Geostatistics

## 1. Introduction

The coarse fluvial deposits of the alpine forelands, e.g. river valleys in Switzerland, France and Austria, are important groundwater aquifers for municipal

water supplies. Natural heterogeneities of these sediments, including sedimentary structures and textures, result in heterogeneities of the hydraulic, chemical and biological aquifer properties, which control the behavior of groundwater flow and solute transport. For many hydrogeologic problems, e.g. determination of capture zones of wells, river–groundwater interaction, contaminant transport behavior, the knowledge of heterogeneity is crucial (Rauber et al., 1998).

\* Corresponding author. Tel.: +41-61-267-3592; fax: +41-61-267-2998.

E-mail address: peter.huggenberger@unibas.ch (P. Huggenberger).

Information on heterogeneity can be of quite different character and quality: (1) outcrop information (e.g. sedimentological classification) is usually sparse, (2) borehole information (e.g. drill core description, pumping test) provides only a limited view of subsurface properties, and (3) geophysical information (e.g. seismic, ground penetrating radar (GPR or georadar)), although often powerful for delineating sedimentary structures, only provides an indication to possible lithological facies.

The problem of adequately modeling subsurface uncertainties becomes more difficult with increasing heterogeneity. The uncertainty depends both on the quantity and on the quality of available data. The geostatistical technique used to model uncertainty in a specific context should be chosen considering the features of the phenomenon under consideration, the knowledge of the subsurface, and the causes of uncertainty (Ayyub and Gupta, 1997).

Several recent studies have investigated the use of geophysical, borehole, and outcrop data to characterize subsurface sedimentary and hydraulic properties (e.g. Beres and Haeni, 1991; Rubin et al., 1992; Coptly et al., 1993; Huggenberger, 1993; Hyndman et al., 1994; Beres et al., 1995; Coptly and Rubin, 1995; Hubbard et al., 1997; Langsholt et al., 1998; Hubbard et al., 1999; Beres et al., 1999; Asprien and Aigner, 1999; Miller et al., 2000), and to use these data to support groundwater flow and solute transport modeling (e.g. Poeter and McKenna, 1995; McKenna and Poeter, 1995; Hyndman and Gorelick, 1996; Rauber et al., 1998). These studies suggest that high-resolution geophysical data can be helpful delineating aquifer structures as well as estimating hydraulic aquifer properties. As these data typically provide two-dimensional information about the subsurface, conditioned stochastic simulation techniques are commonly used to generate probability distributions of the aquifer properties at locations where no data exist (Deutsch and Journel, 1998; Journel and Huijbregts, 1989, and others). Kunstmann and Kinzelbach (1998) studied several methods to quantify model output uncertainty under given input parameter uncertainty. They considered the stochastic simulation to be the method of choice for almost any quantification of model uncertainties.

The estimation of parameter values at locations without data is very important. The determination of

the conditioning data is very important as well, because the conditioning of stochastic simulations strongly influences the simulation results, e.g. groundwater flow pattern and solute transport behavior (Schafmeister, 1997). In most cases, the conditioning is based on facies analysis. A facies is considered a homogeneous, isotropic or anisotropic unit, which is hydrogeologically relevant for groundwater flow and solute transport (Anderson, 1989). Depending on the data acquisition method, both lithofacies (e.g. from outcrop and/or drill core descriptions) and radarfacies, with corresponding hydraulic properties, can be distinguished.

On the theoretical and computational side, geostatistical techniques and visualization tools are available for the representation of heterogeneity in models; however, techniques which allow the integration of data of different quality to condition geological or groundwater flow and solute transport models are still an area of major research. At the outcrop scale, coarse-grained fluvial deposits have been successfully described in terms of architectural element analysis (Siegenthaler and Huggenberger, 1993) and hydraulic properties (Jussel et al., 1994). A principal finding of these authors was that the coarse-grained fluvial deposits are composed of a limited number of sedimentary structure types, each with characteristic hydraulic properties, e.g. porosity and hydraulic conductivity. Recent research also demonstrates the possibility of complete three-dimensional facies analysis using georadar and outcrop analysis (e.g. Beres et al., 1999). Particular time 'slices' or subhorizontal image surfaces are used as a tool for determining the strikes of inclined layers and for depicting the connectivity and spatial relations of the main sedimentary structure types. In most cases, however, three-dimensional geophysical surveys are not possible because of trees, buildings and installations. Similarly, outcrop analysis is often restricted to a small number of exposures or excavations. In most practical problems, drilling is one of the most commonly used methods to determine aquifer thickness, groundwater table and bedrock surface. However, only limited information on heterogeneity is extracted. Possible causes are: (1) no information on geometry and interconnection of sedimentary structures, (2) main lithofacies responsible for fast water conducts such as open-framework gravel are overlooked, (3) existence

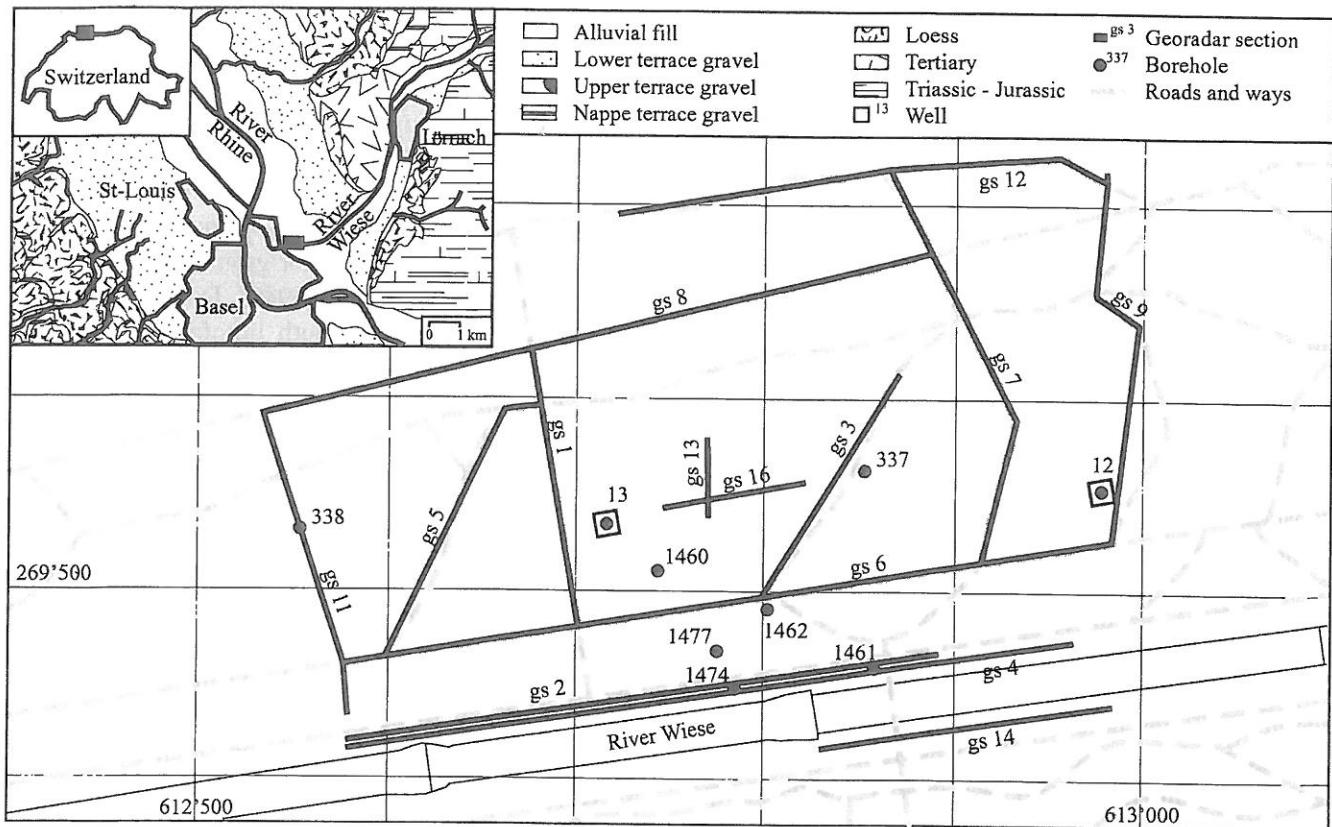


Fig. 1. Geological map of the region of Basel in northwestern Switzerland and map of the test site showing locations of boreholes and traces of georadar sections.

of drill core descriptions of different geologists which cannot easily be integrated into a coherent deterministic concept.

For example, about 3000 drill core descriptions from Basel are stored in a data base (Noack, 1993, 1997). Starting at the beginning of the 20th century, these descriptions often differ from the standard classification systems (e.g. unified soil classification system (USCS)) and important sedimentary structure types, such as the highly permeable open-framework gravel, are generally overlooked due to smearing with overlying and underlying layers during the drilling process. The occurrence and the size of the open-framework gravel, however, determine the variance of the hydraulic conductivity and the correlation length in coarse gravel deposits (e.g. Jussel et al., 1994). For these two reasons, there generally is an important gap between outcrop and drill core descriptions. The strong association of open-framework gravel to the related structure type open-framework/

bimodal gravel couplets (Jussel et al., 1994) has led to the idea that drill core descriptions might also be used to identify sedimentary structure types from older boreholes.

The objective of the present paper is the derivation of a gradual lithofacies-based interpretation of outcrop, drill core and GPR data, which represent data of different quality. The presented method allows a probability estimation of drill core layer descriptions and radarfacies types representing defined sedimentary structure types. The structure type probabilities can be given for points along boreholes and a grid with arbitrary mesh size along georadar sections. The method is applied on field examples from the Rhine/Wiese aquifer near Basel. The resulting structure type probabilities can be used for conditioning stochastic simulations of geological models. However, the conditioned stochastic simulation of the Rhine/Wiese aquifer is the topic of another paper.

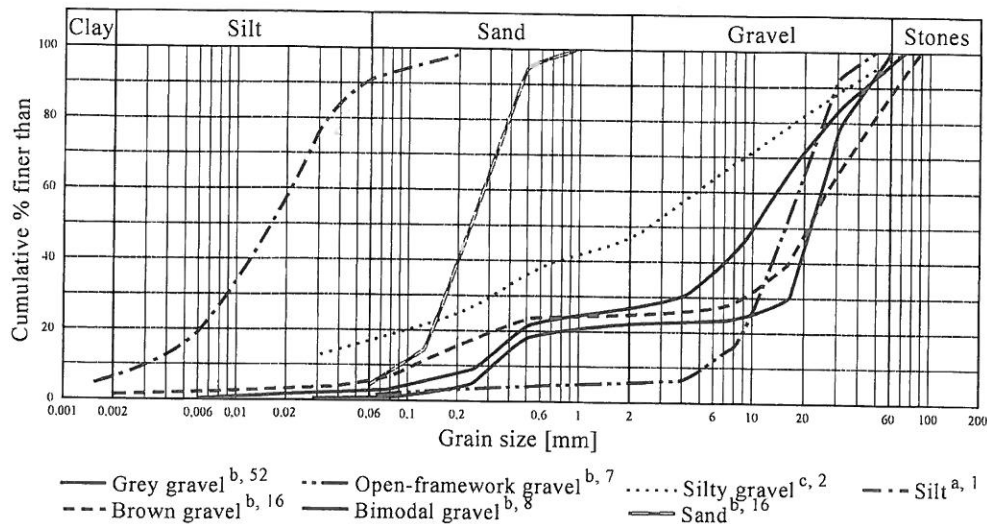


Fig. 2. Typical grain-size distribution (cumulative wt%) of the sedimentary texture types from (a) Huggenberger et al. (1988), (b) Jussel et al. (1994), and (c) Rohrmeier (2000); 52 number of samples.

## 2. Results of field investigations

### 2.1. Sedimentological and hydrological investigations

Heterogeneities of natural gravel deposits in north-eastern Switzerland were investigated in unweathered outcrops by Siegenthaler and Huggenberger (1993), and Jussel et al. (1994). Siegenthaler and Huggenberger (1993) proposed a model of the Pleistocene Rhine gravel aquifer using a limited number of sedimentary structure types based on fluvio-dynamic interpretations of processes in a braided river system. Jussel et al. (1994) examined the sedimentary structure types with a focus on hydraulic parameters.

Outcrop and drill core analyses show that the sedimentary structure types, which are geometric features detectable in the aquifer, are composed of one or two sedimentary texture types. The classification of the sedimentary texture types includes data on grain-size distribution, color and sorting. In literature, the term 'lithofacies' (e.g. Miall, 1996, p. 79, table 4.1) is probably nearest to 'sedimentary texture types'. The sedimentary structure types are defined based on bounding surfaces and fill. The fill may be characterized by the sedimentary texture types and the layering. In the literature, the term 'architectural element' (e.g. Miall, 1996, p. 93, table 4.3) is probably nearest to 'sedimentary structure types'. However, the signifi-

cance of lithofacies and architectural element in literature often differs from author to author.

In general, the sedimentary texture and structure types are easily recognizable in outcrops due to color variations caused by the presence or absence of silt and clay in the gravel, which also results in different water contents. Therefore, color attributes are used for texture type names such as 'gray gravel' or 'brown gravel'. The structure type names are derived from these texture type names. Consequently, the sedimentary structure types comprise gray gravel (GG), brown gravel (BG), alternating gray and brown gravel layers (GG/BG), open-framework gravel (OW), open-framework/bimodal gravel couplets (OW/BM), sand lenses (SA), and silt lenses (SI).

Fig. 1 shows the geological map of the region of Basel in northwestern Switzerland and the test site. In the ancient confluence system of the main river Rhine and its tributary Wiese, the physical processes were expected to be the same as upstream. Therefore, the same sedimentary texture and structure types as described by Siegenthaler and Huggenberger (1993), Jussel et al. (1994), and Rauber et al. (1998) are expected and were actually found. However, the sediments are from different source areas with distinct geological units, which allow a clear assignment of the sediments to the source areas. Due to changing dynamics, caused by the significant widening of the Rhine Valley at Basel, the character of the fluvial



system also include elements, which are typical for the braided-meandering transition (e.g. point-bar deposits). For this reason, the existing lithofacies scheme (Siegenthaler and Huggenberger, 1993) has to be expanded with the new texture type silty gravel (SG), which forms sedimentary structures as well. The distinction of this texture and structure type is based on outcrop and georadar investigations, drill core descriptions, and grain-size analyses. The occurrence of silty gravel may be caused either by the braided-meandering transition of the fluvial system character at Basel, or by the sedimentation of fine material in the backwater of the tributary Wiese, which results from the high discharge in the main river Rhine.

The silty gravel is a very poorly sorted gravel with a sand fraction of nearly 30% and a silt and clay fraction of nearly 20%. The color of the gravel is brownish (Rohrmeier, 2000). The grain-size distribution of the various recurring texture types, which are arranged from the different works to see the heterogeneity of these deposits, are represented in Fig. 2. The variability of the hydraulic aquifer properties of the sedimentary structure types is outlined in Jussel et al. (1994). The compiled data revealed large differences in hydraulic conductivity between the sedimentary structure types (Rauber et al., 1998, p. 2227, table 1).

## 2.2. Geophysical investigations

Sedimentological information from outcrops is usually sparse, and borehole information only provides a limited view of subsurface properties. The georadar technique is a non-destructive geophysical method capable of resolving heterogeneities at the scale of observable sedimentary structures. It allows one to identify the spatial arrangement (e.g. location, geometry and interconnectness) of erosion surfaces separating sedimentological units. The georadar technique turned out to be a powerful tool for mapping sedimentary structures in coarse gravel deposits of the shallow subsurface (up to 20 m).

For the georadar survey in northwestern Switzerland near Basel (Fig. 1), a pulseEKKO IV georadar system with a 1000 V transmitter was used (Sensors and Software Inc., 1993). The transmitting and receiving antennae were separated by 2 m and the step size used was 0.25 m. Tests showed that 50 MHz antennae allow a resolution of the aquiclude surface, the main

erosion boundaries and the larger sedimentary structures to a depth of the aquiclude at approximately 20 m. The excellent penetration depth of electromagnetic waves in these Rhine/Wiese gravel deposits may be explained by the low electrical conductivities of the pore and groundwater (100–150  $\mu\text{S}/\text{cm}$ ).

The vertical resolution depends on the radar-wave frequency of the applied georadar system and is equal to a quarter of the wavelength (Jol and Smith, 1991) and is of the order of 50 cm. According to the theory, reflections of low conductive geological materials occur when electromagnetic waves meet boundaries between lithological units of contrasting dielectric constants. Such reflections can occur either at the change of water content within the same texture type, or at the boundary between two distinct structure types. Due to the low and constant electrical conductivities of the gravel deposits, the influence of electrical conductivity may be neglected for this particular aquifer. Reflection coefficients for the main lithofacies transitions of gravel deposits have been derived for saturated and non-saturated conditions (Huggenberger, 1993). Compared with the results from the 100 and 200 MHz antennae (Huggenberger, 1993; Beres et al., 1999), the erosion surfaces, which separate the main sedimentary structures, and some of the larger internal structures are expected to be resolved. Due to the larger wavelengths of the 50 MHz antennae, only few transitions of alternating sequences of open-framework and bimodal gravels may be portrayed on the georadar sections. The presented example (see Section 3.2, Fig. 6), however illustrates that even the main sedimentary structures may be delineated. Furthermore, it seems that in this particular case, the georadar response of small features (e.g. fine scale bedding), the clutter effects (Annan and Chua, 1988), are minimized. As a consequence, the 50 MHz antennae allow to delineate the significant sedimentological features of coarse, electrically low conductive sediments at the scale of the required model resolution.

In this paper, some examples of two-dimensional georadar surveys conducted in the floodplain of the ancient confluence system of the main river Rhine and its tributary Wiese near Basel are reported. The georadar grid was oriented approximately parallel and perpendicular to the ancient main and tributary flow directions. After acquisition, the georadar data were




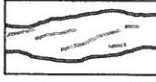

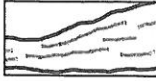

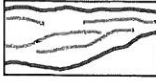

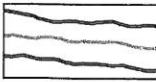
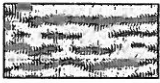
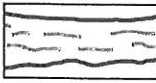

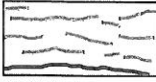


Radarfacies type	Reflection pattern	Interpretation
	(a)	(b)
trough shaped (ts)		
oblique parallel (op)		
oblique tangential (ot)		
oblique sigmoidal (os)		
parallel continuous (pc)		
parallel discontinuous (pd)		
subparallel oblique (so)		
reflection poor (rp)		

Fig. 3. Two-dimensional radarfacies types of coarse gravel deposits as seen in vertical sections, primarily valid for 50 MHz antennae, slightly modified from Beres et al. (1999): (a) reflection pattern, (b) interpreted horizons.

time-zero adjusted. The pairs of linear arrivals in expanding spread soundings (or common midpoint (CMP); Beres et al., 1999), that intersect at zero traveltime and at zero offset, represent the intersection of the air and the groundwave. This point is used to define the reference zeropoint for the different georadar profiles. Further processing steps included trace editing, data merging, bandpass filtering, and automatic gain control with a window of 0 to 500 ns.

Huggenberger (1993), and Beres et al. (1995, 1999) investigated heterogeneities of Rhine gravel deposits in northeastern Switzerland. Different radarfacies types have been distinguished based on established concepts of seismic stratigraphy and radarfacies analysis (e.g. Hardage, 1987; Beres and Haeni, 1991). The radarfacies types observed in vertical sections are trough shaped (ts), oblique parallel (op), oblique tangential (ot), parallel continuous (pc),

parallel discontinuous (pd) and reflection poor (rp). The same radarfacies types could be recognized in the Rhine/Wiese gravel deposits near Basel in north-western Switzerland. At this location, two additional radarfacies types, oblique sigmoidal (os) and subparallel oblique (so), could be distinguished. The distinction of these radarfacies types is based on reflection pattern analysis and the applied georadar system configuration (Rohrmeier, 2000).

The radarfacies types are already described in earlier work (Huggenberger, 1993; Beres et al., 1999). The oblique sigmoidal (os) radarfacies type, which was found in the Rhine/Wiese gravel deposits near Basel, represents sequences that are inclined towards their lower and upper boundary with tangential bottom and top reflections. In the subparallel oblique (so) radarfacies type, which was also found in the Rhine/Wiese gravel deposits, one observes sequences that are subhorizontal, mostly discontinuous and sometimes distinctly inclined layered. The different radarfacies types representing the heterogeneity of these deposits are represented in Fig. 3. They are primarily valid for 50 MHz antennae.

### 3. Interpretation of data

Outcrop, borehole and geophysical information represent data of different quality and scale. Due to the easy access to undisturbed sedimentary structures and textures, outcrop and laboratory investigations of representative samples provide the most reliable, hard data. However, only few outcrops are available for study.

Drilling destroys the microfabric and smears the boundaries of adjacent layers. A drill core layer description is typically not very detailed and does not clearly indicate an explicit texture or structure type, even if a grain-size analysis is available (e.g. overlapping ranges of grain-size distribution of different sedimentary texture types; Jussel, 1992, p. 40, figs. 2.5a–d). Furthermore, the individual drill core descriptions vary considerably between geotechnical and sedimentological aspects. Pumping tests provide conductivity data, which represent mean values averaged over relatively large volumes. They do not provide definite information on geometry and dimensions of subsurface structures. Therefore, drill core and pumping test data are considered soft data.

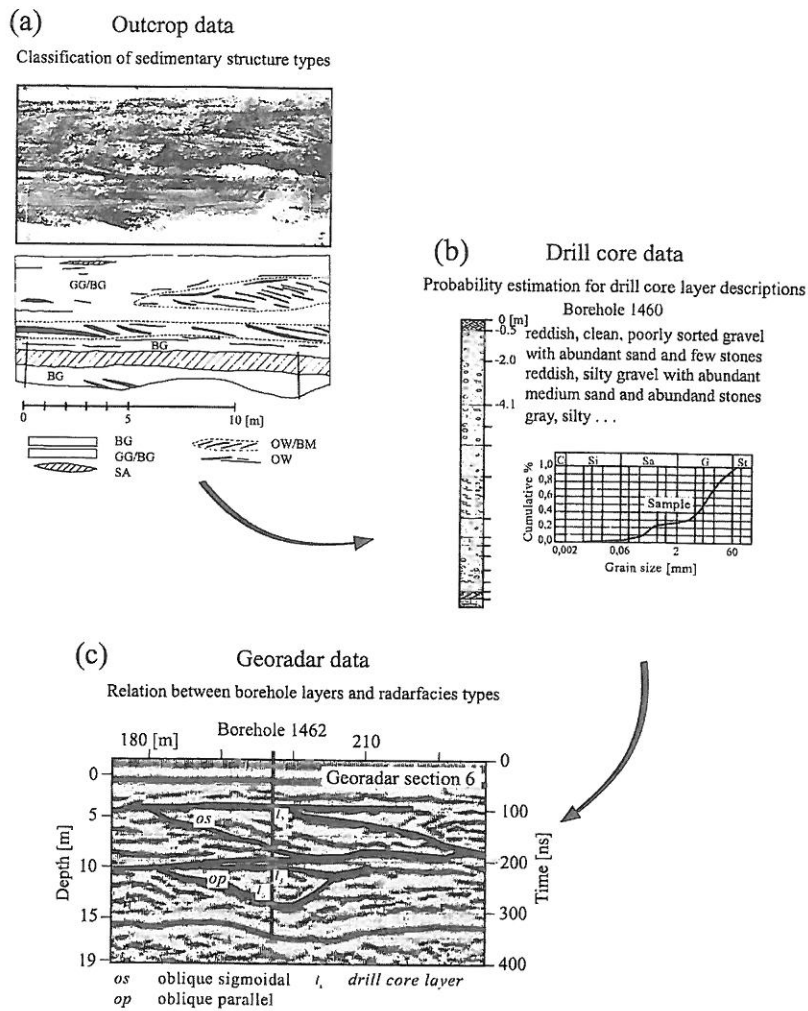


Fig. 4. Interpretation of data of different quality and scale: (a) classification of the sedimentary structure types from outcrop data (Siegenthaler and Huggenberger, 1993; Jussel et al., 1994; Rohrmeier, 2000), (b) probability estimation of correct classification based on drill core layer description, and (c) relation between borehole layers and corresponding radarfacies types.

With the non-destructive georadar technique, sedimentary structures can be delineated. The relationship between reflection patterns and sedimentary structure types is often ambiguous. The reflection patterns only provide an indication to possible sedimentary structure types. Since georadar data are more uncertain than drill core data, they are subsequently considered soft data.

The following interpretation of data of different quality and scale is qualitatively illustrated in Fig. 4. For this interpretation, three steps are necessary. In a first step, the sedimentary structure types were classified from outcrop data (Siegenthaler and Huggenberger, 1993; Jussel et al., 1994; Rohrmeier, 2000; Fig. 4(a)). In a second step, for drill core data, the

probability of correct classification is estimated based on layer descriptions (see Section 3.1; Fig. 4(b)), and in a last step, drill core layers and corresponding radarfacies types are related (see Section 3.2; Fig. 4(c)).

### 3.1. Interpretation of drill core data

Sedimentological drill core descriptions primarily include information on grain size, but also 'additional information' such as main constituent, quantity, fraction, and sorting of single grain-size categories, color; chemical precipitation, layer thickness, and adjacent layer. Based on this additional information, the probabilities of representing specific sedimentological

Table 1

Typical grain-size distribution (cumulative wt%) of the sedimentary structure types: OW: open-framework gravel, OW/BM: open-framework/bimodal gravel couplets, GG: gray gravel, BG: brown gravel, GG/BG-horizontal: alternating gray and brown gravel, horizontally layered, GG/BG-inclined: alternating gray and brown gravel, inclined, SG: silty gravel, SA: sand, SI: silt

Grain-size category	Sedimentary structure type								
	OW	OW/BM	GG	BG	GG/BG		SG	SA	SI
					Horizontal	Inclined			
Silt (and clay)	1	1	3	6	5	5	17	4	91
Sand	6	15	27	25	27	27	48	100	100
Gravel	100	100	97	88	93	93	98		
Stones			100	100	100	100	100		

structure types, which are defined by outcrop data (Siegenthaler and Huggenberger, 1993; Jussel et al., 1994; Rohrmeier, 2000) can be differentiated. If further additional information is available, the probability that a layer description represents a specific sedimentary structure type (structure type probability) increases. The estimation of the structure type probabilities for a drill core layer description is obtained in two steps.

In a first step, grain-size categories, mentioned in drill core layer descriptions are used for an initial

probability estimation. This is done by a (1) determination of average grain-size distribution for the structure types which are then used for an (2) estimation of 'initial structure type probabilities': (1) Most sedimentary structure types are composed of one single texture type with the exception of open-framework/bimodal gravel couplets and alternating gray and brown gravel layers, which can be inclined or layered horizontally. Bimodal gravel itself does not represent a structure type. Based on the grain-size distribution of the different texture types (Fig. 2), grain-size

Table 2

Initial sedimentary structure type probabilities (%) for grain-size categories and combinations thereof grouped according to the number of constituents in a drill core layer description

Grain-size category	Sedimentary structure type								
	OW	OW/BM	GG	BG	GG/BG		SG	SA	SI
					Horizontal	Inclined			
Silt	1	1	2	5	3	3	13	3	69
Sand	2	6	10	8	9	9	13	39	4
Gravel	19	17	15	13	13	13	10	0	0
Stones	0	0	9	37	23	23	8	0	0
Silt, sand	1	3	6	6	6	6	13	23	36
Silt, gravel	10	9	8	9	8	8	11	2	35
Silt, stones	0	0	6	21	13	13	10	2	35
Sand, gravel	11	12	12	10	11	11	11	20	2
Sand, stones	1	3	10	22	16	16	10	20	2
Gravel, stones	9	9	12	25	18	18	9	0	0
Silt, sand, gravel	7	8	9	8	9	9	12	14	24
Silt, gravel, stones	7	6	9	18	13	13	10	1	23
Sand, gravel, stones	7	8	12	19	15	15	10	13	1
Silt, sand, stones	1	2	7	16	12	12	11	15	24
Silt, sand, gravel, stones	5	6	9	16	12	12	11	11	18



Table 3

Additional information in drill core layer descriptions and the relative weighting factor  $w_{relative}$  [ ] with indication of the sedimentary structure type, for which the additional information is typical. The color separation above and below  $-5.0$  m arises from the different geology of the source areas: above  $-5.0$  m the deposits consists exclusively of Wiese gravels, below  $-5.0$  m the deposits consists of Rhine and Wiese gravels

Additional information (Iteration number)	Typical sedimentary structure types	Relative weighting factor ( $w_{relative}$ )
(1) <i>Main constituent</i>		1
Silt	SI	
Sand	SA	
Gravel	OW, OW/BM, GG, BG, GG/BG-h/-i, SG	
(3) <i>Quantity of (clay)-silt-(sand)</i>		0.7
Clean	OW, OW/BM, GG, GG/BG-h/-i, SA	
Few silt/silty	BG, GG/BG-h, GG/BG-i, SA	
Few silt and sand	OW, OW/BM	
Much silt/clayish	SG	
(4) <i>Quantity of sand</i>		0.7
Few sand, 3–15%	OW/BM, BG, SG, SI	
Abundant sand, 16–30%	GG, BG, GG/BG-h/-i, SG	
Much sand, 31–49%	GG, SG, SA	
(10) <i>Quantity of gravel</i>		0.25
Few gravel, 3–15%	SA, SI	
Abundant gravel, 16–30%	SA, SI	
Much gravel, 31–49%	SA, SI	
(11) <i>Quantity of stones</i>		0.25
Few stones	OW/BM, GG, BG, GG/BG-h/-i, SG, SA	
Abundant stones	GG, BG, GG/BG-h/-i	
Much stones	BG	
(5) <i>Fraction of sand</i>		0.55
Fine sand	BG, GG/BG-h/-i, SA, SI	
Medium sand	OW/BM, GG, BG, GG/BG-h/-i, SG, SA	
Coarse sand	OW/BM, GG, SA	
(8) <i>Fraction of gravel</i>		0.4
Fine gravel	GG, SG, SA, SI	
Medium gravel	OW, OW/BM, GG, GG/BG-h/-i, SA	
Coarse gravel	OW/BM, BG, GG/BG-h/-i	
(2) <i>Open-framework gravel</i>		0.85
Open-framework gravel	OW, OW/BM	
Fe-/Mg-precipitation	OW, OW/BM	
(6) <i>Sorting of sand</i>		0.55
Well sorted	OW/BM, GG, SA	
Poorly sorted	OW, BG, GG/BG-h/-i, SG, SA	
(9) <i>Sorting of gravel</i>		0.4
Well sorted	OW, OW/BM, SA	
Poorly sorted	GG, BG, GG/BG-h/-i, SG, SA	
(7) <i>Color (above <math>-5.0</math> m)</i>		0.55
Gray	OW, OW/BM, GG	
Brown	GG, BG, SG, SA, SI	
Gray–brown	GG, BG, GG/BG-h/-i, SG, SA, SI	
(7) <i>Color (below <math>-5.0</math> m)</i>		0.55
Gray	OW, OW/BM, GG, SG, SA, SI	
Brown	BG	
Gray–brown	GG/BG-h/-i, SA	

Table 3 (continued)

Additional information (Iteration number)	Typical sedimentary structure types	Relative weighting factor ( $w_{relative}$ )
(12) <i>Thickness of layer</i>		0.25
Thin, <0.25 m	OW	
Normal, 0.25–2.5 m	OW/BM, GG, BG, GG/BG-h/i, SG, SA, SI	
Thick, >2.5 m	BG	
(13) <i>Adjacent layer</i>		0.1
SA	SI	
OW, OW/BM, GG	BG, GG/BG-h/i, SG	
BG, GG/BG-h/i, SI, SG	OW, OW/BM, GG, SA	

distribution for the structure types are derived (Table 1). This is done as follows: for the structure types composed of one single texture type, the grain-size distribution is identical. For the structure types composed of two texture types, the grain-size distribution was determined by the arithmetic mean of the contents of the grain-size categories. (2) Based on the values in Table 1, the initial structure type probabilities for grain-size categories and combinations thereof are derived (Table 2). This is done as follows: the structure type probabilities for the single grain-size categories are determined by the normalization of the grain-size distribution values over all structure types. The structure type probabilities for combinations of grain-size categories are determined by the arithmetic mean of the structure type probabilities of the single grain-size categories.

In a second step, additional information from the drill core layer descriptions, listed in Table 3, is used for the further differentiation of the sedimentary structure type probabilities. Each kind of additional information is typical for a subset of sedimentary structure types and is given a relative weighting factor  $w_{relative} = ]1; 0.1[$ . The relative weighting factor is estimated based on the significance of the additional information for determining a specific structure type, and on the relative importance of the structure type for groundwater flow and solute transport. A relative weighting factor of 1 is given for a strong association with a given kind of additional information, a relative weighting factor of 0.1 is given for a weak one. The differentiation of the sedimentary structure type probabilities follows an iterative process, where each kind of additional information is considered using the

following equation:

$$P_{st,l,i} = P_{st,l,i-1} W_{st,l,i,ai\pm} \quad (1)$$

where  $P_{st,l,i}$  are the probabilities of the sedimentary structure types ( $st = 1, \dots, m$ ) for a drill core layer description ( $l = 1, \dots, o$ ) after an iteration ( $i = 1, \dots, p$ ). The probabilities of the structure types of the preceding iteration  $P_{st,l,i-1}$ , for which the additional information ( $ai = 1, \dots, n$ ) is typical ( $ai +$ ), are multiplied with the weighting factor  $W_{st,l,i,ai+}$ . The probabilities of the structure types of the preceding iteration, for which the additional information is not typical ( $ai -$ ), are multiplied with the weighting factor  $W_{st,l,i,ai-}$ . This notation is summarized in the factor  $W_{st,l,i,ai\pm}$ . The weighting factors are expressed as follows:

$$W_{st,l,i,ai+} = \left( \frac{100}{\sum_{st=1}^m P_{st,l,i-1,ai+}} \right)^w \quad (2)$$

$$W_{st,l,i,ai-} = 1 + \frac{\sum_{st=1}^m P_{st,l,i-1,ai+} (1 - W_{st,l,i,ai+})}{\sum_{st=1}^m P_{st,l,i-1,ai-}} \quad (3)$$

where  $\sum_{st=1}^m P_{st,l,i-1,ai+}$  is the sum of the probabilities of those structure types of the preceding iteration for which the additional information presently taken into account

is typical; while  $\sum_{st=1}^m P_{st,l,i-1,ai-}$  is the sum of the probabilities of those structure types of the preceding iteration for which the additional information presently taken into account is not typical. To ensure that the sum of the structure type probabilities equals 100 after each iteration (Eq. (1)), a normalization is included in Eq. (2), while Eq. (3) is related to Eq. (2). The exponent

$$w = w_{\text{relative}} c \quad 0 < w < 1 \quad (4)$$

contains both the relative weighting factor of the additional information and the factor representing the general confidence in the drill core description  $c = ]0.9; 0.1[$ . A factor of confidence of 0.9 is given for high confidence in the drill core description (e.g. due to detailed drill core analysis based on the USCS and additional sedimentological details). A factor of confidence of 0.1 is given for little confidence in the drill core description (e.g. due to bad drill core analysis or wash drilling).

Various types of weighting factors (e.g. general form  $x, x^y$ , etc. for  $W_{st,l,i,ai+}$ ;  $W_{st,l,i,ai-}$  is related to  $W_{st,l,i,ai+}$ ) were tested with 56 drill core descriptions from five drill cores (Fig. 1, boreholes 1460, 1461, 1462, 1474, 1477) to push a strong and balanced differentiation between the structure type probabilities during the iteration process. The weighting factors in their present forms correspond very well to this criterion (see examples in Section 4.). Because  $W_{st,l,i,ai+} > 1$ , the probability values of the indicated structure types are increased. Because  $W_{st,l,i,ai-} < 1$ , the probability values of the non-indicated structure types are decreased.

The relationship of the parameters  $w_{\text{relative}}$ ,  $c$  and  $W_{st,l,i,ai\pm}$  is illustrated in Fig. 5. If  $\sum_{st=1}^m P_{st,l,i-1,ai+} \ll \sum_{st=1}^m P_{st,l,i-1,ai-}$  (Fig. 5(a)), the weighting factor  $W_{st,l,i,ai+}$  can become very large depending on the choice of  $w_{\text{relative}}$  and  $c$ . Consequently, the probability of the indicated structure types increases significantly with additional information. At the same time, the weighting factor  $W_{st,l,i,ai-}$  becomes only a little smaller than 1, and therefore, the probability values of the structure types which are not indicated, decrease only slightly. The opposite happens if  $\sum_{st=1}^m P_{st,l,i-1,ai+} \gg \sum_{st=1}^m P_{st,l,i-1,ai-}$  (Fig. 5(c)). In this case, the weighting factor  $W_{st,l,i,ai-}$  becomes very small and the probability of the structure types which are not indicated, decreases significantly with additional information. At the same time, the weighting factor  $W_{st,l,i,ai+}$  becomes only a little larger than 1 and, therefore,

the probability values of the indicated structure types increases only slightly. A balance occurs when  $\sum_{st=1}^m P_{st,l,i-1,ai+} \approx \sum_{st=1}^m P_{st,l,i-1,ai-}$  (Fig. 5(b)).

### 3.2. Interpretation of georadar data

Georadar data (e.g. reflection profiles) provide two-dimensional images allowing subdivision of the subsurface into zones between prominent reflections with different reflection patterns. According to the interpretation concepts of Hardage (1987), and Beres and Haeni (1991), a radarfacies type may be defined as a mappable, three-dimensional sedimentary structure with a reflection pattern differing from those in adjacent structures. The geometry of these structures can be delineated by (1) the more continuous reflections, and (2) the types of reflection patterns within a certain visible structure. In addition, an angular unconformity between prominent reflections can be an indicator of an erosional surface, which separates different sedimentary structures. Because automated selection of reflections produces poor results, manual selection is preferred.

Transformation of the reflections from traveltime to depth requires information on the velocity distribution. The velocity field of the georadar waves is derived from CMPs. Semblance velocity analysis (e.g. Beres et al., 1999) shows interval velocities between 7 and 11 cm/ns (mean at 9.5 cm/ns) for the different CMPs. Depending on the velocity field, linear or more complex velocity functions have to be considered for the transformation of the reflections from traveltime to depth. Due to the accuracy of the vertical resolution (0.5 m) and the variance of the wave velocity in comparison with the resolution of the lithological units in drill cores (0.5 m), a constant velocity is acceptable in a first step. For more complex velocity functions, calibration curves transforming individual boundaries from two-way traveltime to depths including interpolation schemes for differing neighboring velocity logs have to be considered (Coptly and Rubin, 1995).

The radarfacies types (Fig. 3) are calibrated with the interpreted drill cores located in the vicinity of the georadar sections. The calibration process consists of the assignment of the calculated sedimentary structure type probabilities from the drill core layer descriptions (see Section 3.1) to the

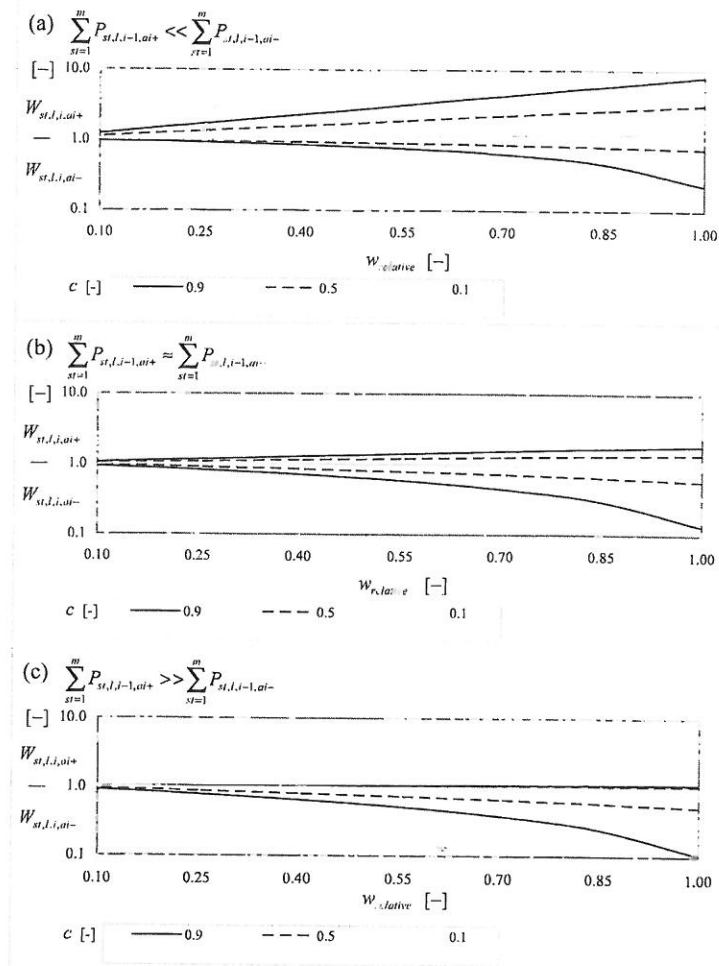


Fig. 5. Influence of additional information from drill core layer descriptions on the differentiation of sedimentary structure types. Relationship between the relative weighting factor of additional information  $w_{relative}$  [ ], the factor taking into account the general confidence in the drill core description  $c$  [ ], and the weighting factors  $W_{st,l,i,ai+}$  [ ] and  $W_{st,l,i,ai-}$  [ ], which are used for the calculation of the sedimentary structure type probabilities in an iterative process: (a) The sum of the probabilities of those structure types of the preceding iteration for which the additional information is typical ( $\sum_{st=1}^m P_{st,l,i-1,ai+}$ ) is much smaller than the sum of the probabilities of those structure types for which the additional information is not typical ( $\sum_{st=1}^m P_{st,l,i-1,ai-}$ ), (b) the corresponding sums of the structure type probabilities of the preceding iteration are approximately equal, (c) the sum of the probabilities of those structure types of the preceding iteration for which the additional information is typical is much larger than the sum of the probabilities of those structure types for which the additional information is not typical. Note the logarithmic scale of the y-axis.

corresponding radarfacies types using the following equation:

$$P_{st,rf} = \sum_{l=1}^s P_{st,l} \frac{h_l}{h_{rf}} \quad (5)$$

where  $P_{st,rf}$  is the probability of the sedimentary structure types ( $st = 1, \dots, m$ ) for a reflection pattern of a defined radarfacies type ( $rf = 1, \dots, q$ ). The structure type probabilities of those drill core layers, which are

part of the georadar structure ( $l = 1, \dots, s$ ), are added according to the proportion in thickness between the drill core layer and the georadar structure ( $h_l/h_{rf}$ ). If the thickness of the drill core layer is equal to or larger than the one of the georadar structure, an adjustment of the structure type probabilities is superfluous. Fig. 6 shows this relation for the oblique sigmoidal and the oblique parallel radarfacies types with a portion of the georadar section 6 and the borehole 1462 (Fig. 1). The differences in thickness of drill core layers and georadar



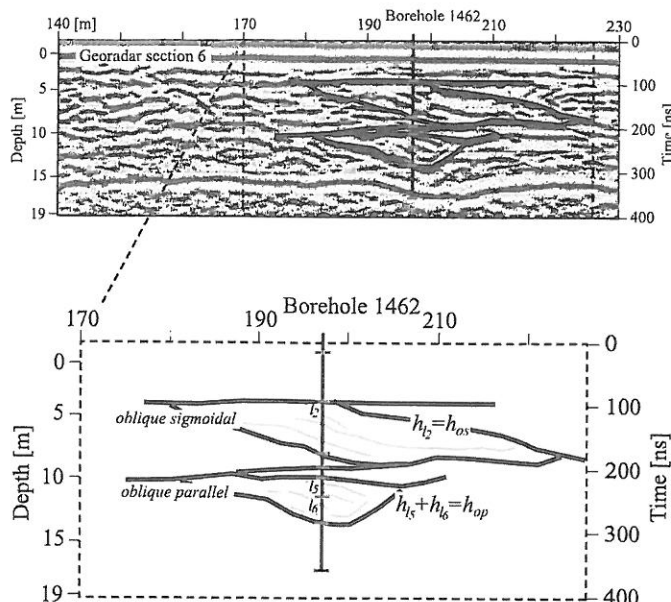


Fig. 6. Assignment of the sedimentary structure type probabilities from the drill core layer descriptions to the corresponding radarfacies types according to the proportion in thickness between the drill core layer and the georadar structure; here shown for the oblique sigmoidal and the oblique parallel radarfacies types within a portion of georadar section 6 (gs 6) and borehole 1462 located in this section.

structures depend on the discrepancy of the resolution accuracy between the visual drill core analysis (few centimeters) and the frequency-dependent georadar mapping (e.g. for 50 MHz antennae few decimeters).

### 3.3. Transformation of reflection patterns into point data

For the application of georadar data in subsurface modeling, the two-dimensional images of georadar sections have to be transferred into point data. Data processing is necessary, once facies analysis is performed. The processing of the available data is schematically illustrated in Fig. 7 and consists of (a) digitizing reflection pattern boundaries, (b) snapping common points of neighboring polygons (georadar structures), (c) gridding polygons and generating nodes (gridpoints), (d) transforming relative into absolute coordinates, and (e) assigning data to nodes.

The digitization of the reflection patterns ( $rp = 1, \dots, r$ ) is carried out with digicps-3, an appended digitizing software for CPS-3 (Radian Corporation, 1992). Usually, the points of neighboring polygons are not coincident. For the successive data processing steps, supplemental program routines were written in C. The snapping tool allows the input of the radius ( $r$ )

in which polygon points shall be snapped. The gridding tool allows the input of the area of the georadar section ( $A = a_1, a_2, z_1, z_2$ ) to be gridded and the input of the horizontal (mh) and vertical (mv) mesh sizes between nodes. Nodes ( $n = 1, \dots, s$ ) with the same  $a$ -coordinates but various  $z$ -coordinates are grouped into a 'georadar borehole' ( $gd = 1, \dots, t$ ). The data density has to be chosen in a way that georadar structures are clearly shown. The coordinate transformation tool changes relative two-dimensional coordinates ( $a, z$ ) into absolute three-dimensional coordinates ( $x, y, z$ ). Finally, the assigning tool allows the arrangement of all information like data source (georadar or borehole), borehole number, node number,  $x$ -,  $y$ - and  $z$ -coordinates, depth, polygon number, reflection pattern number, detail whether surface node or not, probabilities of the sedimentary structure types OW, OW/BM, GG, BG, GG/BG-h, GG/BG-i, SG, SA, SI, and RO (rock) to the corresponding nodes. The data are in a comma-separated-value (csv) format, with each node in a separate line and each kind of information separated by a comma. Subsurface modeling software requires spatial coordinates ( $x, y, z$ ) as well as data like sedimentary structure types, probability details, hydraulic and geotechnical parameters, etc. obtained at the nodal location.

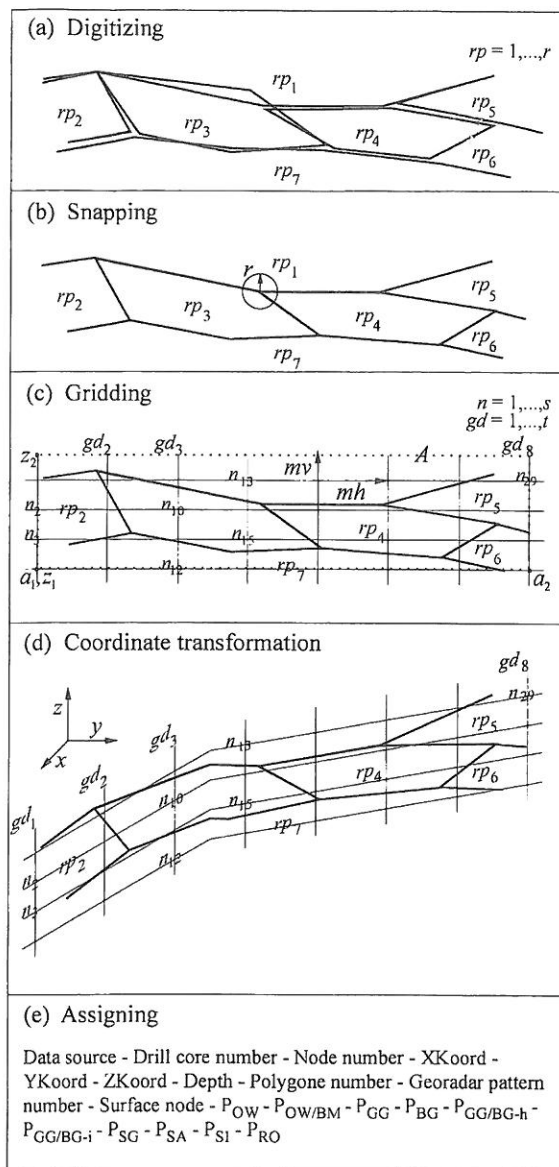


Fig. 7. Transformation of reflection patterns into point data: (a) digitizing of georadar pattern boundaries; (b) snapping of common polygon points; (c) gridding of polygons and generating nodes (gridpoints); (d) transformation of relative into absolute coordinates; (e) assigning of data to nodes.

#### 4. Examples, results and discussion

##### 4.1. Differentiation of sedimentary structure types from drill core layer descriptions

The differentiation of the sedimentary structure types by the method presented in Section 3.1 is shown with two examples. Example 1: For instance, the description of layer 5 from borehole 1477 (Fig. 1)

— clean, poorly sorted gravel with abundant medium and coarse sand and abundant stones, brown appearance, normal thickness, and a lower layer of rather silty gravel types — contains several kinds of additional information (Table 3), which allow the differentiation of individual structure type probabilities. Starting with the probability values for ‘sand, gravel, stones’ (Table 2, line 13), the subsequent iterations (Fig. 8) lead to a variably strong differentiation of the structure type probabilities depending on the additional information and the factor of confidence in the drill core description. The choice of the order of the iterations strongly affects the intermediate probabilities, but has almost no effect on the final probability values, as shown with fine vertical lines.

Example 2: Various orders of additional information were studied using 56 drill core layer descriptions from boreholes 1460, 1461, 1462, 1474, and 1477 (Fig. 1). Fig. 9 shows the final mean probabilities of the sedimentary structure types and their absolute deviations after considering all available additional information. An increase in confidence not only leads to a stronger differentiation of the final mean structure type probabilities (y-axis), but also to an increase in the absolute deviation of the final mean structure type probabilities (x-axis). In general, the absolute deviations from the final mean structure type probabilities are smaller than 3% for structure types that are clearly distinguished from each other (Fig. 9(a)).

##### 4.2. Redundancy of the interpretation method

The probability estimation of a drill core layer description representing a specific sedimentary structure type, presented in Section 3.1, includes two steps: (1) the initial probability estimation for grain-size categories and combinations thereof (Table 2), using grain-size distribution of the sedimentary structure types (Table 1), and (2), the further differentiation of the structure type probabilities taking into account the available additional information (Table 3). Consequently, at both steps, information on grain-size distribution is interpreted. The multiple interpretation of this information is reasonable in this case. First, in the case where no additional information is available (e.g. older, scarce drill core descriptions), the initial probability values already represent a discrete

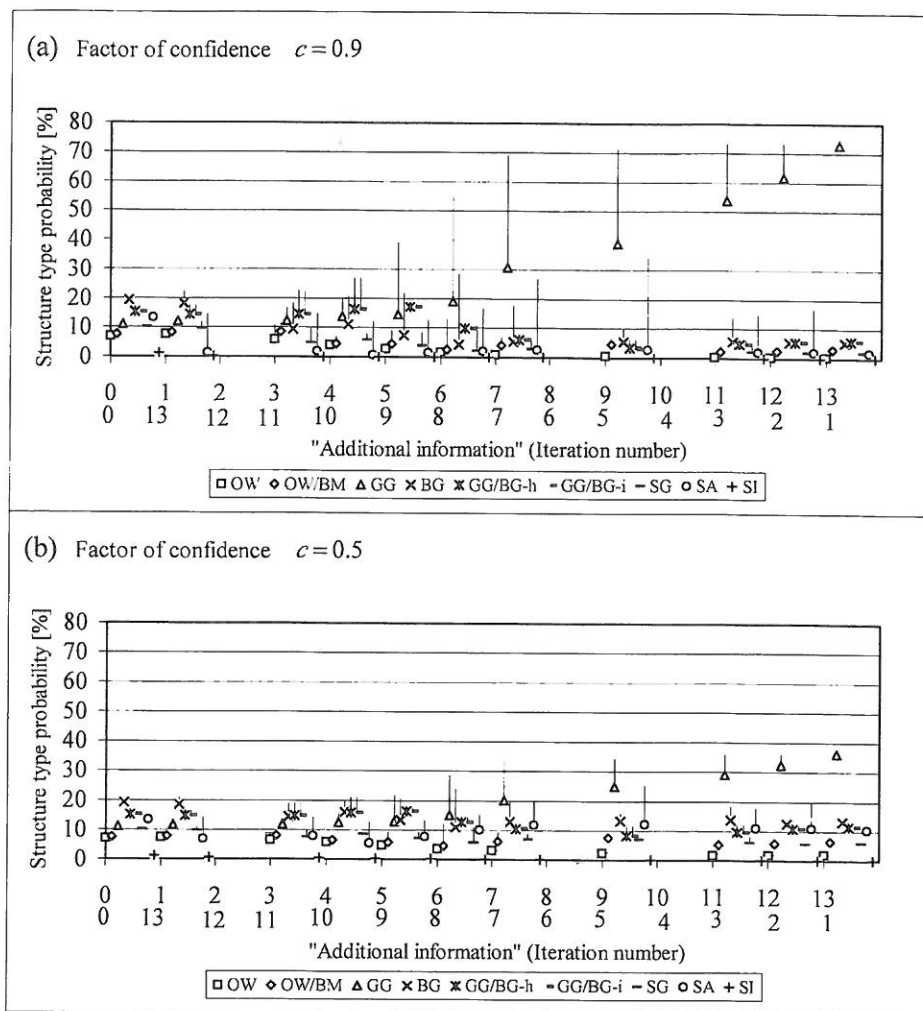


Fig. 8. Differentiation of the sedimentary structure type probabilities (%) based on the order of the additional information and the factor of confidence in the drill core description; shown for layer 5 from borehole 1477. The fine vertical lines indicate the range of the structure type probabilities depending on the order of the additional information taken into account.

differentiation of the structure types. Second, applying the USCS classification, not all additional information concerning the quantity of the different grain-size categories (Table 3) can occur together. In most practical cases, however, the descriptions are not available in such detail.

#### 4.3. Probability matrix for radarfacies types

The assignment of the calculated structure type probabilities to the radarfacies types by the method presented in Section 3.2 leads to a probability matrix (Table 4). This assignment is shown in Fig. 6 for the oblique sigmoidal and the oblique parallel radarfacies types. The matrix also contains an estimate as well as

calculated probability values. The estimate is based on sedimentological considerations and the comparison of georadar patterns with outcrop observations after excavation (Beres et al., 1999).

### 5. Conclusions

Fluvial and glaciofluvial deposits in northwestern Switzerland are strongly heterogeneous. They consist of different, well-defined sedimentary structure types. Depending on the data acquisition method, lithofacies or radarfacies with different features were characterized. Outcrop and laboratory investigations of representative samples concerning hydraulic properties

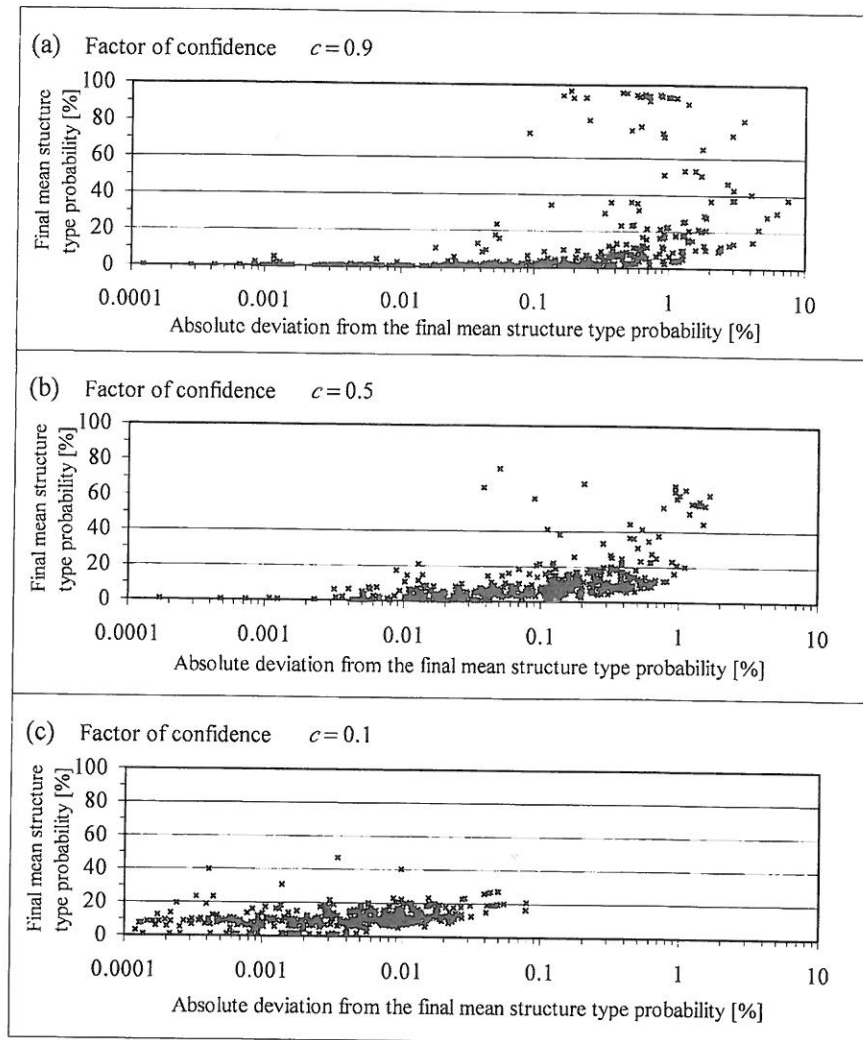


Fig. 9. Final mean probabilities of the sedimentary structure types and their absolute deviations as a function of the order of additional information and the factor of confidence in the drill core description. The data refer to 56 drill core layer descriptions from boreholes 1460, 1461, 1462, 1474, and 1477.

provide the most reliable data, and are considered hard data. Therefore, drill core and georadar data are fuzzy to some extent and are considered soft data. The georadar data are more uncertain than the drill core data with respect to the indication of sedimentary structure types.

The method presented respects these differences of data uncertainty and allows a gradual lithofacies-based interpretation of outcrop, drill core, and georadar data. The lithofacies scheme is based on fluvio-dynamic considerations and is suitable for the interpretation of the radarfacies. The result is a probability estimation of drill core layer descriptions and radarfacies types representing defined sedimentary

structure types. The method includes a determination of initial structure type probabilities for grain-size categories and combinations thereof described in drill core layer descriptions as well as a following differentiation of these structure type probabilities in an iterative process considering additional information like main constituent, quantity, fraction, and sorting of single grain-size categories, color, chemical precipitation, layer thickness, and adjacent layer. The radarfacies types are calibrated with drill cores located in the vicinity of georadar sections. The calibration process consists of the assignment of the calculated structure type probabilities from the drill core layer descriptions to the corresponding



Table 4

Sedimentary structure type probabilities (%) for different radarfacies types. The probability values are given for different factors of confidence in the drill core description, and estimates based on sedimentological considerations and the comparison of georadar patterns with outcrop observations after excavation

Radarfacies type	Sedimentary structure type	Sedimentary structure type								
		OW	OW/BM	GG	BG	GG/BG		SG	SA	SI
						Horizontal	Inclined			
Trough shaped	Estimated	0	50	25	0	0	5	2	15	3
	$c = 0.9$	13	81	1	2	0	0	3	0	0
	$c = 0.5$	16	41	7	9	4	4	9	4	6
	$c = 0.1$	8	10	9	15	11	11	11	10	15
Oblique parallel	Estimated	0	50	20	0	0	8	7	15	0
	$c = 0.9$	8	31	20	7	9	9	15	0	1
	$c = 0.5$	9	16	14	11	11	11	15	6	7
	$c = 0.1$	6	9	11	14	12	12	12	12	12
Oblique tangential	Estimated	0	30	10	0	0	8	30	20	2
	$c = 0.9$	4	21	13	7	5	5	44	0	1
	$c = 0.5$	6	13	10	10	9	9	26	5	10
	$c = 0.1$	6	8	10	13	11	11	13	12	16
Oblique sigmoidal	Estimated	0	7	5	0	0	8	50	25	5
	$c = 0.9$	1	9	4	7	2	2	73	0	2
	$c = 0.5$	4	10	7	12	6	6	37	4	14
	$c = 0.1$	6	7	9	12	10	10	15	11	20
Parallel continuous	Estimated	0	5	25	5	15	0	0	35	15
	$c = 0.9$	0	1	1	0	1	2	0	94	1
	$c = 0.5$	2	6	8	5	6	6	3	64	0
	$c = 0.1$	5	6	12	13	12	12	9	29	2
Parallel discontinuous	Estimated	0	7	35	15	30	0	0	10	3
	$c = 0.9$	1	1	6	37	22	22	9	1	1
	$c = 0.5$	3	4	10	23	17	17	13	7	6
	$c = 0.1$	6	7	9	11	10	10	13	14	20
Subparallel oblique	Estimated	0	2	20	20	35	5	3	15	0
	$c = 0.9$	2	6	24	20	19	19	7	3	0
	$c = 0.5$	4	7	16	18	16	16	9	10	4
	$c = 0.1$	7	8	11	14	13	13	11	12	11
Reflection poor	Estimated	0	0	25	25	15	0	0	25	10
	$c = 0.9$	3	4	6	15	11	11	17	32	1
	$c = 0.5$	5	6	9	15	12	12	12	22	7
	$c = 0.1$	7	8	10	14	13	13	11	10	14

radarfacies types considering the proportion in thickness between drill core layers and georadar structures. The structure type probabilities can be given for points along boreholes and a grid with arbitrary mesh size along georadar sections. The method is applied on field examples from the Rhine/Wiese aquifer near Basel.

The resulting structure type probabilities can be

used for conditioning stochastic simulations of geological models. However, the conditioned stochastic simulation of the Rhine/Wiese aquifer is the topic of another paper.

The results show the importance of a detailed sedimentological analysis of outcrops and drill cores, and its significance on the distinction of sedimentary structure types. The method presented allows

a differentiation between the highly permeable open-framework gravel and open-framework/bimodal gravel couplets, which are only rarely described in the classic literature on coarse braided river stratigraphy. As these sedimentary structure types show a high hydraulic conductivity, act as preferential pathways and therefore strongly influence solute transport behavior. In addition, older outcrop and drill core data can also be interpreted and integrated in the lithofacies scheme.

### Acknowledgements

We thank M. Rohrmeier and P. Schwer for the georadar data acquisition, Th. Noack, C. Miracapillo and E. Zechner for their constructional discussions, L. Rosenthaler and U. Aschauer for their instructions in programming and K. Zechner, H. Einstein and W. Barrash for reviewing the manuscript. We also thank two anonymous reviewers, who have contributed to the improvement of the paper. This study was financially supported by Swiss National Science Foundation Grant 2100-049272.96/1.

### References

- Anderson, M.P., 1989. Hydrogeologic facies models to delineate large-scale spatial trends in glacial and glaciofluvial sediments. *Geological Society of America Bulletin* 101, 501–511.
- Annan, A.P., Chua, L.T., 1988. Ground penetrating radar performance predictions. Pilon, J.A. (Ed.). *Ground Penetrating Radar*. Geological Survey of Canada Paper 90-4.
- Asprion, U., Aigner, T., 1999. Towards realistic aquifer models: three-dimensional georadar surveys of quaternary gravel deltas (Singen Basin, SW Germany). *Sedimentary Geology* 129 (3–4), 281–297.
- Ayyub, B.M., Gupta, M.M., 1997. *Uncertainty Analysis in Engineering and Sciences: Fuzzy Logic, Statistics, and Neural Network Approach*. Kluwer Academic, Dordrecht.
- Beres, M., Haeni, F.P., 1991. Application of ground-penetrating radar methods in hydrogeologic studies. *Ground Water* 29 (3), 375–386.
- Beres, M., Green, A.G., Huggenberger, P., Horstmeyer, H., 1995. Mapping the architecture of glaciofluvial sediments with three-dimensional georadar. *Geology* 23 (12), 1087–1090.
- Beres, M., Huggenberger, P., Green, A.G., Horstmeyer, H., 1999. Using two- and three-dimensional georadar methods to characterize glaciofluvial architecture. *Sedimentary Geology* 129, 1–24.
- Copt, N., Rubin, Y., 1995. A stochastic approach to the characterization of lithofacies from surface seismic and well data. *Water Resources Research* 31 (7), 1673–1686.
- Copt, N., Rubin, Y., Mavko, G., 1993. Geophysical–hydrological identification of field permeabilities through bayesian updating. *Water Resources Research* 29 (8), 2813–2825.
- Deutsch, C.V., Journel, A.G., 1998. *GSLIB Geostatistical Software Library and User's Guide*. Oxford University Press, Oxford.
- Hardage, B.A., 1987. *Seismic Stratigraphy*. Geophysical Press, London.
- Hubbard, S.S., Rubin, Y., Majer, E., 1997. Ground-penetrating-radar assisted saturation and permeability estimation in bimodal systems. *Water Resources Research* 33 (5), 971–990.
- Hubbard, S.S., Rubin, Y., Majer, E., 1999. Spatial correlation structure estimation using geophysical and hydrogeological data. *Water Resources Research* 35 (6), 1809–1825.
- Huggenberger, P., 1993. Radar facies: recognition of facies patterns and heterogeneities within Pleistocene rhine gravels, NE Switzerland. Braided Rivers, Best, C.L., Bristow, C.S. (Eds.). *Geological Society Special Publication* 75, 163–176.
- Huggenberger, P., Siegentaler, C., Stauffer, F., 1988. Grundwasserströmung in Schottern: Einfluss von Ablagerungsformen auf die Verteilung von Grundwasserfließgeschwindigkeit. *Wasserwirtschaft* 78 (5), 202–212.
- Hyndman, D.W., Gorelick, S.M., 1996. Estimating lithologic and transport properties in three dimensions using seismic and tracer data: the Kesterson aquifer. *Water Resources Research* 32 (9), 2659–2670.
- Hyndman, D.W., Harris, J.M., Gorelick, S.M., 1994. Coupled seismic and tracer test inversion for aquifer property characterization. *Water Resources Research* 30 (7), 1965–1977.
- Jol, H.M., Smith, D.G., 1991. Ground-penetrating radar of northern lacustrine deltas. *Canadian Journal of Earth Sciences* 28 (12), 1939–1947.
- Journel, A.G., Huijbregts, C.J., 1989. *Mining Geostatistics*. Academic Press, New York.
- Jussel, P., 1992. *Modellierung des Transports gelöster Stoffe in inhomogenen Grundwasserleitern*. Dissertation. Eidgenössisch Technische Hochschule Zürich.
- Jussel, P., Stauffer, F., Dracos, T., 1994. Transport modeling in heterogeneous aquifers: 1. Statistical description and numerical generation of gravel deposits. *Water Resources Research* 30 (6), 1803–1817.
- Kunstmann, H., Kinzelbach, W., 1998. Quantifizierung von Unsicherheiten in Grundwassermodellen. *Mathematische Geologie* 2, 3–15.
- Langsholt, E., Kitterod, N.O., Gottschalk, L., 1998. Development of three-dimensional hydrostratigraphical architecture of the unsaturated zone based on soft and hard data. *Ground Water* 36 (1), 104–111.
- McKenna, S.A., Poeter, E.P., 1995. Field example of data fusion in site characterization. *Water Resources Research* 31 (12), 3229–3240.
- Miall, A.D., 1996. *The Geology of Fluvial Deposits: Sedimentary Facies, Basin Analysis and Petroleum Geology*. Springer, Berlin.
- Miller, R.B., Castle, J.W., Temples, T.J., 2000. Deterministic and stochastic modeling of aquifer stratigraphy, South Carolina. *Ground Water* 38 (2), 284–295.

- Noack, T., 1993. Geologische Datenbank der Region Basel. *Eclogae Geologicae Helveticae* 86 (1), 283–301.
- Noack, T., 1997. Geologische Datenbank der Region Basel-Konzept und Anwendungen. *Mitteilungen der Schweizerischen Gesellschaft für Boden- und Felsmechanik* 133, 13–18.
- Poeter, E.P., McKenna, S.A., 1995. Reducing uncertainty associated with ground-water flow and transport predictions. *Ground Water* 33 (6), 899–904.
- Radian Corporation, 1992. CPS-3, User's Manual. Radian Corporation, Austin, London.
- Rauber, M., Stauffer, F., Huggenberger, P., Dracos, T., 1998. A numerical three-dimensional conditioned/unconditioned stochastic facies type model applied to a remediation well system. *Water Resources Research* 34 (9), 2225–2233.
- Rohrmeier, M., 2000. Geologische Modelle im Anströmbereich von Wasserfassungen. Diplomarbeit, Universität Basel.
- Rubin, Y., Mavko, G., Harris, J., 1992. Mapping permeability in heterogeneous aquifers using hydrologic and seismic data. *Water Resources Research* 28 (7), 1809–1816.
- Schafmeister, M.T., 1996. Parameter estimation for ground-water models by indicator kriging. *GeoENV I — Geostatistics for Environmental Applications*, Proceedings of the Geostatistics for Environmental Applications Workshop, Lisbon, Portugal, 18–19 November, Soares, A., Gomez-Hernandez, J., Froidevaux, R. (Eds.). *Quantitative Geology and Geostatistics* 9, 165–176.
- Sensors and Software Inc., 1993. PulseEKKO Software user's guide. Sensors and Software Inc., Mississauga, Ontario.
- Siegenthaler, C., Huggenberger, P., 1993. Pleistocene rhine gravel: deposits of a braided river system with dominant pool preservation. *Braided Rivers*, Best, J.L., Bristow, C.S. (Eds.). *Geological Society Special Publication* 75, 147–162.